J Therm Anal Calorim (2010) 100:543–549
DOI 10.1007/s10973-009-0018-3

Effect of MoO_3 additions on the thermal stability and crystallization kinetics of $PbO–Sb_2O_3–As_2O_3$ glasses

K. A. Aly · A. Dahshan · Yasser B. Saddeek

Received: 1 April 2009 / Accepted: 13 May 2009 / Published online: 10 June 2009

Abstract The present paper reports on the effect of MoO_3 on the glass transition, thermal stability and crystallization kinetics for $(40PbO–20Sb_2O_3–40As_2O_3)_{100-x}–(MoO_3)_x$ ($x = 0$, 0.25, 0.5, 0.75 and 1 mol%) glasses. Differential scanning calorimetry (DSC) results under non-isothermal conditions for the studied glasses were reported and discussed. The values of the glass transition temperature (T_g) and the peak temperature of crystallization (T_p) are found to be dependent on heating rate and MoO_3 content. From the compositional dependence and the heating rate dependence of T_g and T_p, the values of the activation energy for glass transition (E_g) and the activation energy for crystallization (E_c) were evaluated and discussed. Thermal stability for $(40PbO–20Sb_2O_3–40As_2O_3)_{100-x}–(MoO_3)_x$ glasses has been evaluated using various thermal stability criteria such as ΔT, H_r, H_g and S. Moreover, in the present work, the $K_r(T)$ criterion has been considered for the evaluation of glass stability from DSC data. The stability criteria increases with increasing MoO_3 content up to $x = 0.5$ mol%, and decreases beyond this limit.

Keywords Crystallization kinetics · Oxide glasses · Thermal stability

K. A. Aly (✉) · Y. B. Saddeek
Physics Department, Faculty of Science, Al-Azhar University, P.O. Box 71452, Assiut, Egypt
e-mail: kamalaly2001@Gmail.com

A. Dahshan
Department of Physics, Faculty of Science, Suez Canal University, Port Said, Egypt

Introduction

During the last few decades, antimony-lead based glasses have been shown to be of interest from both academic and technological points of view. These glasses were found to be insoluble in water or nitric and sulphuric acids and suitable for potential applications in non-linear optical devices like broad band optical amplifiers operating around 1.5 μm [1–4] and in a number of solid state ionic devices since these glasses possess large non-linear optical susceptibility (χ^3) coefficient [5]. The latter physical property may be manifest itself from the deformability of the lone pair of electrons of the structural unit SbO_3 of Sb_2O_3 which can be viewed as tetrahedrons with the oxygen at three corners and a lone pair of electrons at the fourth corner localized in the third equatorial direction of Sb atom [6–8].

On the other hand, it was established that, ions of molybdenum have high activity and selectivity in a series of oxidation reactions in the different oxide glasses which are considered to be good candidates for the study of catalytic properties [9–11]. Syam Prasad et al. [11] supposed that molybdenum oxide has a dual role in glass-forming matrices; it is an incipient glass network former and does not readily form the glass but does so in the presence of the modifier oxides like PbO with MoO_4^{2-} structural units and it may also act as modifier with MoO_6 and $Mo^{5+}O$ structural groups [12, 13]. Shah et al. [14] in a study on some alkali lead borophosphate glasses showed that these glasses possess low T_g, higher thermal expansion coefficient, and at low Na_2O content, the glass may be suitable for glass-to-metal seal with Cu–Be alloys. Melting temperatures as observed on high temperature microscope were found to be matching with those of DTA studies within acceptable limits. This type of information is quite important for deciding intimate contact with metal and the dwell time for

fabrication of seal, which in turn controls the inter-diffusion at the interface.

Different simple quantitative methods have been suggested in order to evaluate the level of stability of the glasses. Some of them are based on the characteristic temperatures [15, 16], and some depend on the activation energy for crystallization [17, 18]. The characteristic temperatures such as the glass transition temperature (T_g), the onset temperature of crystallization (T_c), the temperature corresponding to the maximum crystallization rate (T_p), and the melting temperature of crystalline phase (T_m) are easily and accurately obtained by the differential scanning calorimetry [19] during the heating processes of the glass sample.

Dietzel introduced the first glass criterion, $\Delta T = T_c - T_g$, to evaluate the glass-forming ability of the glasses. By the use of the characteristic temperatures, Hruby developed the H_r criterion, $H_r = \Delta T/(T_m - T_p)$, and the compositional dependence of the Hruby coefficient were surveyed by Sestak [20]. On the basis of the H_r criterion, Saad and Poulain [21] obtained two other criteria, weighted thermal stability criterion $H_g = \Delta T/T_g$ and $S = (T_p - T_c)\Delta T/T_g$.

In the present work, the effect of addition of MoO_3 (0, 0.25, 0.5, 0.75 and 1 mol%) on the thermal stability and crystallization kinetics for the new $(40PbO–20Sb_2O_3–40As_2O_3)_{100-x}–(MoO_3)_x$ glasses is investigated. The above-mentioned criteria have been applied to the present glasses. In addition, a kinetic parameter, $K_r(T)$, with an Arrhenian temperature dependence, is introduced to the stability criteria.

Experimental details

In the present study, $(40PbO–20Sb_2O_3–40As_2O_3)_{100-x}–(MoO_3)_x$ ($x = 0$, 0.25, 0.5, 0.75 and 1 mol%) glasses have been prepared with the conventional glass melting technique. Appropriate amounts of reagent grades of PbO, Sb_2O_3, As_2O_3 and MoO_3 were mixed thoroughly in an agate mortar and melted in a covered platinum crucible in an electrically heated furnace under ambient atmospheric conditions at temperature about 1,073 K for 1 h to homogenize the melt. Glasses in frits form were produced by quenching of glass melts in air.

The non-crystalline nature of the annealed glasses was confirmed by X-ray diffraction using a Philips X-ray diffractometer PW/1710 with Ni-filtered Cu-Kα radiation ($\lambda = 1.542$ Å) operating at 40 kV and 30 mA. The patterns (not shown) revealed broad humps characteristic of the amorphous materials and did not reveal discrete or any sharp peaks.

The calorimetric measurements were carried out using a differential scanning (Shimadzu 50 with an accuracy of ±0.1 K) calorimeter. The calorimeter was calibrated, for each heating rate, using well-known melting temperatures and the melting enthalpies of zinc and indium supplied with the instrument. The glass powder (after crushing them into powder form) weighing 20 mg were contained in an aluminum crucible and the reference material was α-alumina powder. The samples were heated in air at uniform heating rates ($\alpha = 4$, 8, 16, 24 and 32 K min^{-1}). The values of the characteristic temperatures (T_g, T_c, T_p and T_m) were determined with an accuracy of ±1 K.

Theoretical background

The theoretical basis for interpreting kinetic data is provided by the formal theory of transformation kinetics. This theory describes the evolution with time (t) of the volume fraction crystallized (χ) by Johnson, Mehl and Avrami equation [22]:

$$\chi = 1 - \exp(-(kt)^n) \tag{1}$$

where n is an integer or half integer depends on the mechanism of growth and the dimensionality of the crystal, k is the effective (overall) reaction rate constant, which obeys an Arrhenius expression for the absolute temperature:

$$k(T) = k_0 \exp\left(-\frac{E}{RT}\right) \tag{2}$$

where k_0 is the frequency factor, T is the absolute temperature and E is the effective activation energy describing the overall crystallization process [22–24]. Thus, it easy to deduce the Kissinger formula in the form of;

$$\ln\left(T_p^2/\alpha\right) = E_c/RT_p - \ln(k_0R/E) \tag{3}$$

where E_c is the activation energy for crystallization and the quoted approximation might introduce a 3% error in the value of E_c/R in the worst cases. For crystallization processes with spherical nuclei, it has been suggested [22, 23] that the dependence of the glass transition temperature on α may be written as:

$$\ln\left(T_g^2/\alpha\right) = E_g/RT_g + \text{const.} \tag{4}$$

where E_g is the activation energy for glass transition and R is the gas constant.

In order to evaluate the thermal stability of glassy materials, Surinach et al. [25] and Hu and Jiang [26] introduced two criterion $k(T_g) = k_0 \exp(-E/RT_g)$ and $k(T_p) = k_0 \exp(-E/RT_p)$ respectively. Thus, the values of these two parameters indicate the tendency of glass to devitrify on heating. The larger their values, the greater are the tendency to devitrify. The formation of glass is a

kinetic process, so, it is reasonable to assess the glass stability by a kinetic parameter, $k(T)$ taking in to account, the H_r parameter as;

$$k_r(T) = k_0 \exp\left(\frac{-H_r E}{RT}\right) \quad (5)$$

where T is any temperature between T_g and T_p. The theoretical background for the definition of the parameter $k_r(T)$ would be based on the analysis of the relation between the parameters $k(T)$ and $k_r(T)$. Differentiating Eqs. 2 and 5 with respect to temperature and rewrite each parameter per Kelvin we get:

$$\frac{\Delta k_r}{k_r \Delta T} = \frac{H_r E}{RT^2} \quad \text{and} \quad \frac{\Delta k}{k \Delta T} = \frac{E}{RT^2} \quad (6)$$

The above mentioned variation of the parameter $k_r(T)$ is H_r times the variation in parameter $k(T)$, which could justify the accuracy of the parameter $k_r(T)$. Just like the $k(T)$ criteria, the smaller the values of $k_r(T)$, the greater is thermal stability of the glass. The obvious advantage of this method is that it can evaluate the glass stability over a wide temperature range.

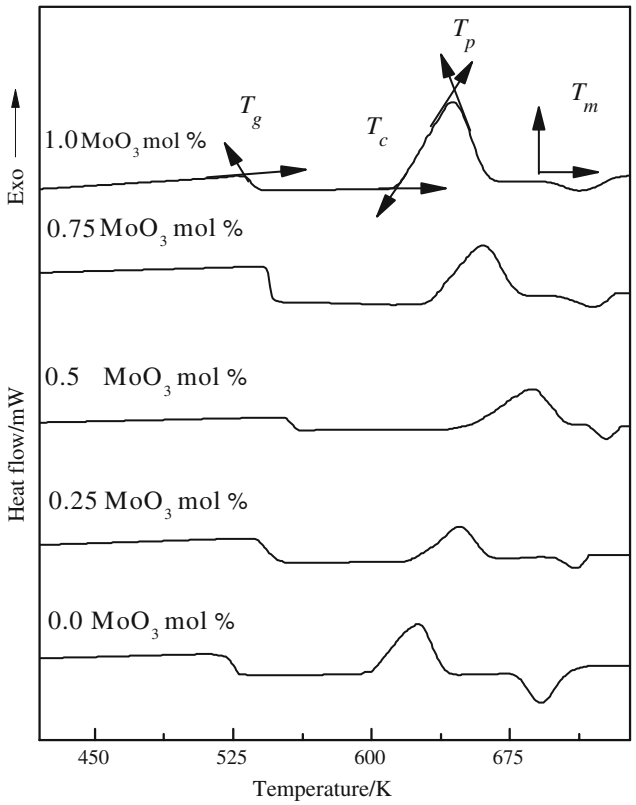

Fig. 1 Typical DSC traces with the characteristic temperatures (T_g, T_c, T_p, and T_m) for $(40PbO–20Sb_2O_3–40As_2O_3)_{100-x}–(MoO_3)_x$ ($x = 0$, 0.25, 0.5, 0.75 and 1 mol%) glasses recorded at heating rate 8 K/(60 S)

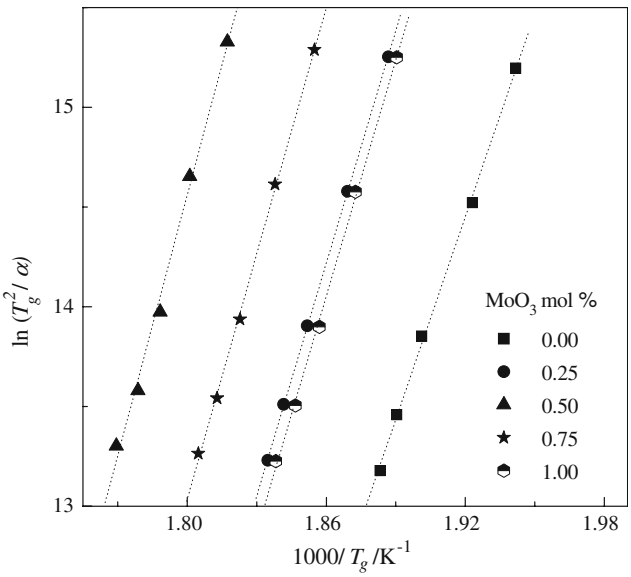

Fig. 2 $\ln(T_g^2/\alpha)$ versus $1000/T_g$ for $(40PbO–20Sb_2O_3–40As_2O_3)_{100-x}–(MoO_3)_x$ glasses (α in second)

Results

Thermal analysis

Figure 1 shows the compositional dependence of the DSC curves including the characteristic temperatures (T_g, T_c, T_p, and T_m) for the studied glasses recorded at a heating rate 8 K min^{-1}. It is clear that, the whole glasses exhibit a single endothermic peak attributed to the glass transition temperature range which represents the strength or rigidity

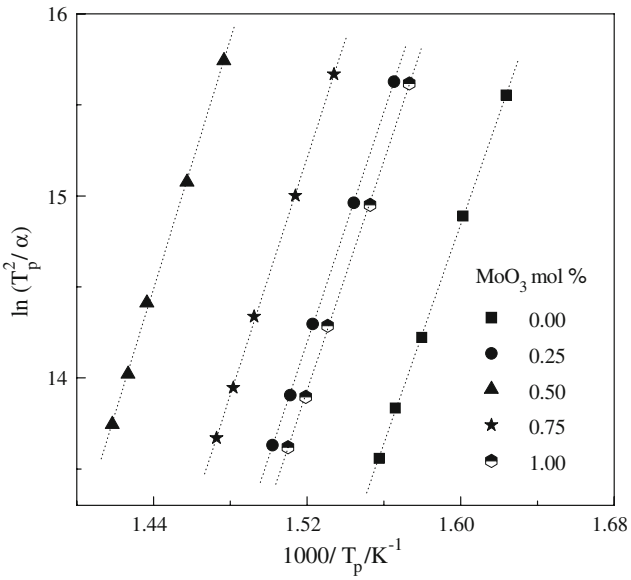

Fig. 3 $\ln(T_p^2/\alpha)$ versus $1000/T_p$ for $(40PbO–20Sb_2O_3–40As_2O_3)_{100-x}–(MoO_3)_x$ glasses (α in second)

of the glass structure. At higher temperatures, there is a single exothermic peak attributed to the full crystal growth. The last peak has two characteristic points: the first is the onset temperature of crystallization (T_c) and the second is the peak temperature of crystallization (T_p). This exothermic peak was followed by another endothermic effect attributed to the melt of the crystalline phase which is denoted by T_m. The appearance of a single peak due to the glass transition temperature in DSC pattern indicates the high homogeneity of the studied glasses. It is found that, the characteristic temperatures (T_g, T_c, T_p and T_m) increase with increasing the MoO_3 content up to 0.5 mol%, and decrease beyond this limit. The analysis of the glass transition temperature dependence on the heating rate (α) will be performed in terms of Eq. 4 to obtain the activation energy for glass transition (E_g), as shown in Fig. 2. From the experimental data, a plot of $\ln(T_p^2/\alpha)$ has been drawn for different compositions showing a straight regression line. From the heating rate dependence of T_g and T_p, (Figs. 2, 3 respectively), the values of the activation energy for glass transition (E_g) and the activation energy for crystallization (E_c) are evaluated and their composition dependence is depicted in Fig. 4. Accordingly, both E_g and E_c increase with increasing MoO_3 content up to $x = 0.5$ mol% and decrease beyond this limit.

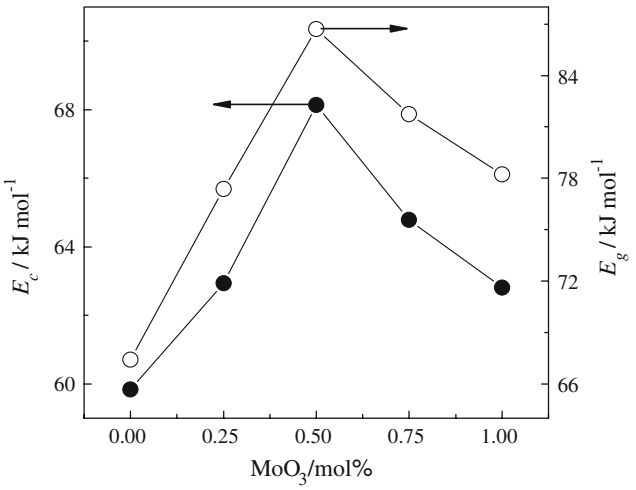

Fig. 4 Activation energies for glass transition (E_g) and for crystallization (E_c) as a function of MoO_3 content for $(40PbO–20Sb_2O_3–40As_2O_3)_{100-x}–(MoO_3)_x$ ($x = 0$, 0.25, 0.5, 0.75 and 1 mol%) glasses

Table 1 The values of T_g, T_c, T_p, T_m and thermal stability criteria (ΔT, H_r, H' and S) for the different heating rates for $(40PbO–20Sb_2O_3–40As_2O_3)_{100-x}–(MoO_3)_x$ ($x = 0$, 0.25, 0.5, 0.75 and 1 mol%) glasses

x (mol%)	α (K min^{-1})	T_g (±1) (K)	T_c (±1) (K)	T_p (±1) (K)	T_m (±1) (K)	ΔT (±1) (K)	H_r	H_g	S (K)
0.0	4	515	589	616	670	74	1.367	0.144	3.858
	8	520	596	625	680	76	1.368	0.146	4.167
	16	526	604	633	690	78	1.381	0.148	4.300
	24	529	608	639	696	79	1.382	0.149	4.570
	32	531	611	642	700	80	1.385	0.151	4.673
0.25	4	530	611	639	689	81	1.616	0.153	4.261
	8	535	618	648	699	83	1.621	0.155	4.578
	16	540	624	657	708	84	1.635	0.156	5.078
	24	543	628	662	714	85	1.642	0.157	5.278
	32	545	631	666	718	86	1.647	0.158	5.488
0.5	4	550	640	677	713	90	2.461	0.163	6.089
	8	555	647	686	723	92	2.477	0.165	6.487
	16	559	654	696	734	95	2.481	0.169	7.165
	24	562	659	701	740	97	2.486	0.172	7.243
	32	565	663	705	744	98	2.498	0.173	7.296
0.75	4	539	624	652	698	85	1.838	0.158	4.343
	8	544	631	661	708	87	1.841	0.160	4.679
	16	549	638	670	718	89	1.848	0.163	5.238
	24	552	642	675	724	91	1.852	0.165	5.363
	32	554	646	679	728	92	1.856	0.166	5.489
1.0	4	528	608	636	689	80	1.503	0.151	4.238
	8	533	615	644	698	82	1.501	0.153	4.506
	16	538	621	653	709	84	1.509	0.155	5.018
	24	541	626	658	714	85	1.512	0.157	5.142
	32	543	629	662	719	86	1.515	0.158	5.266

Thermal stability

The thermal stability for $(40PbO–20Sb_2O_3–40As_2O_3)_{100-x}$ –$(MoO_3)_x$ ($x = 0$, 0.25, 0.5, 0.75 and 1 mol%) glasses can be estimated in terms of the stability criteria parameters ΔT, H_r, H_g and S which are based on the characteristic temperatures of the glasses (Table 1). The variation of ΔT, H_r, H_g and S criteria with the concentration of MoO_3 shows a maximum value at $x = 0.5$ mol%. These observations indicate that the glass at $x = 0.5$ mol% has the highest resistance against crystallization, the highest glass-forming ability and is the most stable one.

Discussion

Thermal analysis

According to the single peak of the full crystallization, there is one most probable crystalline phase can be detected. According to the ICDDVIEW 2006 identification cards [27], the phase can be identified as $AsSbO_4$ which crystallizes in monoclinic system with lattice parameters $a = 4.79$ nm, $b = 6.93$ nm, $c = 5.3$ nm and volume of the unit cell = 175.85 Å^3.

The increase in E_g with the increase in MoO_3 content up to 0.5 mol% may be attributed to the higher bond strength of MoO_3 relative to that of PbO, Sb_2O_3, and As_2O_3 [28], and to the higher coordinated structural unit MoO_6 compared with PbO_4, SbO_3, and AsO_6. The raise in E_g values suggests the former role of MoO_3 with creating bridging oxygens up to 0.5 mol%. Beyond this limit, the former role may be converted into a modifier role with the creation of non bridging oxygens which decrease the E_g values. The former/modifier role of MoO_3 on the lead arsenate glasses was discussed earlier [14]. According to the resemblance of the physical properties of MoO_3 and WO_3 [29], so, it is expected that their effect on the same glassy matrix may be the same. Little Flower et al. [4] studied the role of increasing WO_3 content in lead arsenate antimony glasses and found a similar behavior to our study.

The trend of E_c can be attributed to the difference in the ionic radii of Mo^{6+} and its coordination with oxygens with the ionic radii and coordination with oxygens of Sb_2O_3,

Table 2 The $K(T_g)$, $K_r(T_g)$, $K(T_p)$ and $K_r(T_p)$ criteria for different heating rates for $(40PbO–20Sb_2O_3–40As_2O_3)_{100-x}$–$(MoO_3)_x$ ($x = 0$, 0.25, 0.5, 0.75 and 1 mol%) glasses

x (mol%)	α (K min^{-1})	$K(T_g)/10^{-8} \pm 1\%$	$K(T_p)/10^{-2} \pm 1\%$	$K_r(T_g)/10^{-16} \pm 1\%$	$K_r(T_p)/10^{-11} \pm 1\%$
0.0	4	37	0.53	1.876	8.873
	8	65	1.04	3.639	20.517
	16	126	1.98	4.482	27.880
	24	174	3.00	6.331	45.532
	32	215	3.85	7.500	58.002
0.25	4	19.8	0.52	2.124×10^{-8}	29.222×10^{-6}
	8	34.6	1.00	3.845×10^{-8}	65.797×10^{-6}
	16	59.8	1.97	4.284×10^{-8}	104.311×10^{-6}
	24	82.7	2.86	4.881×10^{-8}	137.581×10^{-6}
	32	102.0	3.82	5.091×10^{-8}	172.438×10^{-6}
0.5	4	4.264	0.497	1.438×10^{-31}	4.213×10^{-24}
	8	7.448	0.957	2.082×10^{-31}	9.395×10^{-24}
	16	11.551	1.962	4.770×10^{-31}	45.162×10^{-24}
	24	15.989	2.743	7.886×10^{-31}	81.298×10^{-24}
	32	22.056	3.639	8.771×10^{-31}	94.168×10^{-24}
0.75	4	14.8	0.510	1.582×10^{-13}	3.422×10^{-10}
	8	25.9	0.985	3.650×10^{-13}	9.875×10^{-10}
	16	42.3	1.982	5.887×10^{-13}	25.283×10^{-10}
	24	58.3	2.818	8.602×10^{-13}	40.613×10^{-10}
	32	76.0	3.754	11.084×10^{-13}	56.894×10^{-10}
1.0	4	21.084	0.5249	1.852×10^{-20}	0.750×10^{-13}
	8	36.937	0.9969	4.701×10^{-20}	2.116×10^{-13}
	16	60.638	2.0074	6.519×10^{-20}	4.293×10^{-13}
	24	84.000	2.8761	8.501×10^{-20}	6.134×10^{-13}
	32	109.908	3.8562	10.746×10^{-20}	8.299×10^{-13}

PbO, and As_2O_3. Little Flower et al. [4] reported that PbO enters the glass network by breaking up the As–O–As, Sb–O–As bonds and introduces coordinate defects known as dangling bonds along with non-bridging oxygen ions. However, PbO may be participated in the glass network with PbO_4 structural units when lead ion is linked to four oxygens in a covalent bond configuration. On the other hand, the ionic radii of Pb^{2+}, Sb^{3+}, As^{3+}, and Mo^{3+} are 91.5, 90, 72, and 73 pm, respectively [29]. Thus, the increase of MoO_3 content up to 0.5 mol% into PbO–Sb_2O_3–As_2O_3 glass matrix may strengthen its structure as it occupy structural glass-forming positions. This occupancy may be due to its small ionic radii and its higher cross-link density. Beyond $x = 0.5$ mol%, there will be a gradual conversion of MoO_6 structural unit into MoO_4 structural unit in the glass network which act as a modifier. So, the structure will be weakened, and the trend to crystal formation will be decreased. The decrease in E_c trend is in accordance with previous work [30].

Thermal stability

The kinetic parameters $K(T)$ and $K_r(T)$ of the studied glasses were calculated according to Eq. 6. These calculations were carried out in order to compare the stability sequence of the studied materials from the quoted parameters with the corresponding sequence deduced from the stability criteria based on the characteristic temperatures. The values of $K(T_g)$, $K_r(T_g)$, $K(T_p)$ and $K_r(T_p)$ for the temperatures T_g and T_p are listed in Table 2. Their data indicates also, that the glass at $x = 0.5$ mol% is the most stable one. Accordingly, one can notice that, the $K_r(T)$ at $x = 0.5$ mol% varies slowly with increasing the temperature, indicating a relatively high stability, while $K_r(T)$ varies more rapidly with increasing T for the other glasses, indicate less stability.

Conclusions

The addition of MoO_3 at the expense of Pbo–Sb_2O_3–As_2O_3 glasses results in an apparent increase in the characteristic temperatures (T_g, T_c, T_p and T_m), the activation energy for glass transition and the activation energy for crystallization up to $MoO_3 = 0.5$ mol%. Beyond $x = 0.5$ mol%, there will be a remarkable decrease in these parameters. This behaviour was attributed to former/modifier role of MoO_3. The thermal stability for these glasses has been evaluated by using various criteria. The results of the criteria K(T_g), $K_r(T_g)$, $K(T_p)$ and $K_r(T_p)$ agree satisfactorily with the other criteria ΔT, H_r, H_g and S for the studied glasses. Based on results of the thermal stability criteria, the glass at $x = 0.5$ mol% is the most stable one.

Acknowledgment The authors wish to thank Al-Azhar University for the financial support.

References

1. Nalin M, Poulain M, Ribeiro JL, Messaddeq Y. Antimony oxide based glasses. J Non-Cryst Solids. 2001;284:110–6.
2. Poirier G, Poulain M, Poulain M. Copper and lead halogeno-antimoniate glasses. J Non-Cryst Solids. 2001;284:117–22.
3. Fargin E, Berthereau A, Cardinal T, Le Flem G, Ducasse L, Canioni L, et al. Optical non-linearity in oxide glasses. J Non-Cryst Solids. 1996;203:96–101.
4. Little Flower G, Sahaya Baskaran G, Krishna Mohan N, Veeraiah N. The structural role of tungsten ions in PbO–$Sb_2$2O_3–As_2O_3 glass-system by means of spectroscopic investigations. Mater Chem Phys. 2006;100:211–6.
5. Terashima K, Hashimoto T, Uchino T, Yoko T. Structure and nonlinear optical properties of Sb_2O_3-B_2O_3 binary glasses. J Ceram Soc Jpn. 1996;104:1008–14.
6. Wells A. Structural inorganic chemistry. 4th ed. Oxford: Clarendon Press; 1975. p. 88.
7. Cotton FA, Wilkinson G, Murillo CA, Bochmann M. Advanced inorganic chemistry. New York: Wiley; 1999. p. 493.
8. Sabadel JC, Armand P, Cachau-Herreillat D, Baldeck P, Doclot O, Ibanez A, et al. Structural and nonlinear optical characterizations of tellurium oxide-based glasses: TeO_2–BaO–TiO_2. J Solid State Chem. 1997;132:411–9.
9. Iordanova R, Dimitrov V, Klissurski D. Glass formation and structure of glasses in the V_2O_5–MoO_3–Bi_2O_3 system. J Non-Cryst Solids. 1994;180:58–65.
10. Klissurski D, Pesheva Y, Abadjeva N. Multicomponent oxide catalysts for the oxidation of methanol to formaldehyde. Appl Catal. 1991;77:55–66.
11. Syam Prasad P, Raghavaiah BV, Balaji Rao R, Laxmikanth C, Veeraiah N. Dielectric dispersion in the PbO–MoO_3–B_2O_3 glass system. Solid State Commun. 2004;132:235–40.
12. Pal M, Hirota K, Sakata H. The dc electrical conductivity of semiconducting TeO_2-V_2O_5-MoO_3. J Phys D Appl Phys. 2001; 34:459–64.
13. El-Hofy M, Hager IZ. Ionic conductivity in MoO_3-BaF_2-AgI-LiF glasses. Phys Status Solidi A. 2000;182:697–707.
14. Shah KV, Goswami M, Aswal DK, Shrikhande VK, Gupta SK, Kothiyal GP. Effect of Na_2O/K_2O substitution on thermophysical properties of PbO based phosphate glasses. J Therm Anal Calorim. 2007;89:153–7.
15. Dahshan A, Aly KA, Dessouky MT. Thermal stability and activation energy of some compositions of Ge–Te–Cu chalcogenide system. Philos Mag. 2008;88:2399–410.
16. Hruby A. Evaluation of glass-forming tendency by means of DTA. Czechoslov J Phys B. 1972;22:1187–93.
17. Marotta A, Buri A, Branda F. Structure and devitrification behaviour of sodium, lithium and barium borophosphate glasses. J Non-Cryst Solids. 1987;95:593–9.
18. Zhao X, Sakka S. Glass formation and crystallization in alkali-containing fluoride glasses. J Non-Cryst Solids. 1987;95:487–94.
19. Borisova ZU. Glassy semiconductors. New York: Plenum; 1981. p. 231.
20. Sestak J. Heat as manufacturing power or the source of disorder? J Therm Anal. 2002;69:113–24.
21. Saad M, Poulain M. Glass forming ability criterion. Mater Sci Forum. 1987;19:11–8.
22. Johnson WA, Mehl KF. Reaction kinetics in processes of nucleation and growth. Trans Am Inst Mining Metall Eng. 1932; 135:416–42.

23. Mahadevan S, Giridhar A, Singh AK. Calorimetric measurements on as-sb-se glasses. J Non-Cryst Solids. 1986;88:11–34.
24. Matusita K, Komatsu T, Yokota R. Kinetics of non-isothermal crystallization process and activation energy for crystal growth in amorphous materials. J Mater Sci. 1984;19:291–6.
25. Surinach S, Baro MD, Clavaguera-Mora MT, Clavaguera N. Glass formation and crystallization in the $GeSe_2$-Sb_2Te_3 system. J Mater Sci. 1984;19:3005–12.
26. Young D, Jiang Z. Relationship between regions of glass formation and pseudoeutectic regions. Phy Chem Glasses. 1990; 31:161–5.
27. ICDD View 2006 Release. Cards No. 00-018-0755, 01-074-0054, 01-077-0295, 00-022-0421, 00-024-0668.
28. Lide D. CRC handbook of chemistry and physics. 84th ed. Boca Raton: CRC Press; 2004. p. 9–52.
29. http://www.webelements.com.
30. Shaaban ER, Shapaan M, Saddeek YB. Structural and thermal stability criteria of $Bi_2O_3–B_2O_3$ glasses. J Phys Condens Matter. 2008;20:155108–17.